Assembly of Gold Nanoparticles into Chiral Superstructures Driven by Circularly Polarized Light

Ji-Young Kim[1,2,‡], **Jihyeon Yeom**[1,3,‡], **Heather Calcaterra**[1,4], **Gongpu Zhao**[5,6], **Peijun Zhang**[5,7,8], **Nicholas Kotov**[1,2,3,4,9]

[1]Biointerfaces Institute, University of Michigan, Ann Arbor, MI, 48109, USA;

[2]Department of Materials Science, University of Michigan, Ann Arbor, MI, 48109, USA;

[3]Macromolecular Science and Engineering, University of Michigan, Ann Arbor, MI, 48109, USA;

[4]Department of Chemical Engineering, University of Michigan, Ann Arbor, MI, 48109, USA;

[5]Department of Structural Biology, University of Pittsburg, Pittsburg, PA, USA;

[6]David Van Andel Advanced Cryo-Electron Microsocpy Suite, Van Andel Research Institute, Grand Rapids, MI 49503, USA;

[7]Division of Structural Biology, Wellcome Trust Centre for Human Genetics, University of Oxford, Oxford, OX3 7BN, UK

[8]Electron Bio-Imaging Centre, Diamond Light Source, Harwell Science and Innovation Campus, Didcot OX11 0DE, UK

[9]Michigan Center for Integrative Research in Critical Care, University of Michigan, Ann Arbor, MI, 48109, USA

Abstract

Photon-to-matter chirality transfer offers both simplicity and universality to chiral synthesis but its efficiency is typically low for organic compounds. New pathways for imposing chiral bias during chemical process are essential for a variety of technologies from medicine to informatics as well as for fundamental science. Strong optical activity of inorganic nanoparticles (NPs) afford photosynthetic routes to chiral superstructures using circularly polarized photons. Plasmonic NPs are especially promising candidates for such reactions but realization and adequate interpretation of light-driven synthesis of chiral nanostructures in light-driven processes was more challenging than for semiconductor NPs. The process also requires unconventional approaches for the quantification of chiral products. Here we show that illumination of nanoscale colloidal dispersions with circularly polarized light induces the formation of chiral nanostructures 10–15 nm in diameter. Despite their seemingly irregular shape, the resulting nanocolloids showed circular dichroism (CD) spectra with opposite polarity after exposure to photons with left- and right circular polarization. The sign and spectral position of the experimental CD peaks of

Corresponding Author: kotov@umich.edu.
‡These authors contributed equally.

illuminated dispersions correlated well with those calculated for assembled nanostructures with complex geometry, as established by transmission electron tomography images. Quantification of the complex shapes of NP assemblies using chirality measures revealed direct correlation of three different indices with the experimental spectra. The mechanism of the light-driven assembly of chiral nanostructures is based on the asymmetric displacement of NPs in dynamic assemblies by plasmonic fields followed by particle-to-particle attachment. The ability of gold nanostructures to retain the polarization information of incident photons can be used to create a variety of chiral nanomaterials with plasmonic resonances.

Chiral compounds have overarching importance for physics, chemistry, and biology.[1–4] Despite the large variety of chemical reactions selective for specific enantiomers, the chemical path to products with mirror asymmetry is typically based on matter-to-matter chiral bias. Chirality transfer from photons to matter[5,6] has both fundamental and practical importance, as a process that could be, for example, involved in explaining the emergence of biomolecular homochirality,[7] employed as a preparative method for chiral compounds,[8,9] and lead to new photonic devices.[10] Some enantiomeric excess *of* small molecules,[11] helical polymers,[12] supramolecular compounds,[5,13] and liquid crystals[6,14,15] after CPL illumination was observed. *H*owever, the enantiomeric excess for the majority of organic and inorganic reactions carried out using CPL is typically small as values of 0.5–2%.[16]

Strong chiroptical activity of inorganic nanostructures associated with high polarizability of inorganic matter[3] offers the possibility of increasing the chiral bias of photoinduced processes. The enantioselective assembly of semiconductor nanoparticles (NPs) by chiral photons was observed for CdTe/CdS nanocolloids and led to the formation of right- and left-handed twisted nanoribbons when, respectively, right- and left-handed light was incident on the NP dispersions.[17] Enantiomeric excess for this photoinduced reaction exceeded 30%.[17,18] Similar processes can potentially be observed for metallic NPs also. However, such processes are difficult to study at the moment, because easily identifiable chiral shapes, such as helices or tetrahedrons familiar from organic chemistry, may not necessarily be dominant for self-assembled nanostructures. Metallic nanoassemblies are often present in far-from-equilibrium states due to strong attractive interactions between them.[3,16,19,20] In fact, some nanoscale assemblies may be geometrically complex and appear achiral while they are not. Furthermore, the attribution of circular dichroism (CD) peaks for inorganic nanostructures can also be polysemous due to multiple optical processes contributing to their optical activity.[3,19,21] Analysis of optical activities of inorganic structures must, therefore, include three-dimensional reconstructions of the synthesized or assembled nanostructures rather than chemical formulas. While tomographic reconstructions of inorganic nanostructures are easier to perform than those for organic nanoscale mater due greater TEM contrast, their acquisition is still far from being high-throughput or routine.

While being mindful of these challenges, there are several factors that make photon-to-matter chirality transfer a promising direction for nanomaterials and, in particular, for plasmonic NPs. First, CPL illumination can potentially influence both the growth and assembly processes of highly polarizable metallic NPs. Hot–electron processes are likely to be both spin-[22] and site-selective[23] leading to asymmetric particle growth. Second, the

assembly processes should also be affected by the coupling of plasmonic and hydrodynamic fields and thus will be CPL-dependent.[24,25] Third, plasmonic NPs are known to be catalytic, [26,27] which makes them suitable for subsequent chirality transfer into other chiral compounds.

In the framework of fundamental and technological importance of asymmetric photosynthesis,[20,28–32] these considerations suggest that self-assembly of gold NPs, driven by circularly polarized photons, will diversify the spectrum and deepen our understanding of light-driven chirality transfer. Here, we demonstrate that CPL induces the formation of chiral Au nanostructures. They have complex shapes that might seem arbitrary but they display preferential handedness nevertheless. CD spectroscopy indicates that gold nanostructures illuminated with left- and right-polarized photons show positive and negative optical activity in the 400–700 nm plasmonic band, respectively. Their 3D geometry was evaluated by electron tomography. Computational models reproduced the polarity of their chiroplasmonic bands. Quantitative analysis of chirality using several chirality measures revealed correlations between their sign/amplitude and CD spectroscopic features.

An aqueous solution (2 mL) of Au(III) chloride hydrate (HAuCl4) and citrate *with* 2.5 mM concentration was illuminated by left- (LCP) or right-handed circularly polarized photons (RCP) at a wavelength of 543 nm. After 50 min of illumination, the formation of pale-yellow dispersions were observed. The dispersions exhibited CD spectra with bands at 550 nm, characteristic of plasmonic resonances in Au NPs (Fig. 1A and B).

The shapes of nanostructures found in dispersions after CPL illumination using transmittance electron microscopy (TEM) can be described as complex 3D structures comprised of several assembled NPs (Fig. 1C and D). To the best of our knowledge, this is the first reported example of using CPL and metal ion solution to synthesize chiral metal NPs. Previous study of photo-induced transformation of plasmonic NPs reported transformation of spherical Ag NPs into racemic prism-like shapes under illumination with white unpolarized light.[33,34]

To elucidate the mechanism of formation and chirality transfer from the incident light to the NPs in dispersion, we acquired TEM images and measured CD spectra at various illumination times (Fig. S1). After 5 min of illumination of (HAuCl$_4$) solutions, reduction of Au^{3+} to Au^0 takes place[35] and ~ 2 nm NPs were found (Fig. S1A). With continued illumination, the NPs grew to become 3–5 nm in diameter and coalesce into structures with complex shapes and dimensions of ~ 10–15 nm. Intensity of the CD and UV-Vis absorbance bands at 550 nm increased with the illumination time (Fig. S1, B and C). When linearly polarized light (LPL) was used as the illuminating source (Fig. S2), the pale-yellow dispersion was formed as well. It acquired a red color after 50 min of illumination. No CD bands appeared at any point during this reaction (Fig. S2, A and B). The Au NPs formed after LPL illumination had elongated shapes (Fig. S2C), which confirms transformation of polarization information of light to the geometry of plasmonic assemblies.

Based on these data, the first two steps for formation of chiral Au nanostructures should include (1) partial reduction of Au(III) by citrate to Au(0) clusters photoactive at 543 nm,

and (2) the growth of Au(0) clusters to form about ~3 nm Au NPs via photo-induced reduction(s). The resulting NPs form dynamic assemblies that acquire anisotropic shapes with chiral bias due to the interdependence of the plasmonic and hydrodynamic forces shaping the NP assemblies.[24,25] To examine this mechanism closer, numerical solutions of the three-dimensional vector Maxwell equations based on a finite-element frequency-domain approach (Comsol Multiphysics) were obtained. The forces acting on five neighboring 3 nm gold NPs by three different polarizations of light (linear, right-handed circular, left-handed circular) were calculated (Fig. 2 and Table 1). The integration of Maxwell surface stress tensor showed that NP assemblies with achiral shapes experience out-of-plane twisting forces induced by CPL that drive them to become chiral. The direction of the forces and, thus, the resulting assemblies change their handedness depending on the polarization rotation of the incident photons. When the incident photons are linearly polarized, the out-of-plane torque twisting of the nanoassemblies is not observed (Fig. 2C). The calculated results match well with the experimental TEM observations and spectroscopic data. The resulting dynamic assemblies with chiral disposition of NPs can be locked in shape by NP-NP merger known as oriented attachment and non-classical crystallization processes.[36–38]

The tomography images revealed complex geometries of the nanoassemblies with handedness that was not easily identifiable (Fig. 2, A and B) as opposed to twisted ribbons or helixes.[17,31] To interpret their chiroptical properties, we directly imported tomography coordinates into COMSOL for calculating their CD spectra. Considering that the experimental spectra represent NP dispersions containing a range of various shapes and sizes, calculated spectra of two individual NPs is adequately correlated with the experimental results (Fig. 3c), with respect to the polarity of the CD peaks and their spectral placement. To the best of our knowledge, this is the first realization of calculations of chiroptical properties performed on the true experimental geometry of the nanostructures.

In addition to CD spectra, the chirality of the resulting nanostructures can be enumerated using chirality measures. The latter can be calculated for different molecules including (bio)organic nanoassemblies, such as proteins, based on their atomic formulae, atomic coordinates and bonding patterns (see SI).[39–41] Calculation of chirality measures for inorganic nanostructures present, however, a challenge because their atomic structure is not absolutely consistent from particle to particle. Garzón and co-workers carried out theoretical calculations of the geometry of chiral clusters and their Hausdorff chirality measures (HCM).[42] It is necessary to import experimentally obtained geometries of chiral nanostructures in order to establish the relationship between polarity and amplitude of CD spectra and a chirality measure.

A chiral nanostructure may be uniquely represented by a 3D density map, p*(x,y,z)*, of the inorganic material that was calculated based on the imported tomography coordinates. Various chirality quantification methods could be applicable to nanoscale structures when they are 'coarse-grained' to a set of 'atoms'. To accomplish this, we developed a process to quantitatively convert the *p(x,y,z)* function into an idealized molecule. The center of mass of a NP with an arbitrary shape that will be referred to as primary center of mass, was placed at the (0,0,0) point of the Cartesian coordinate system. The nanostructure was aligned to have its farthest surface point as *z* intercept while *x* intercept represents the farthest in the *xy*

plane. The structure was then sectioned into eight pieces according to octants of the Cartesian system of coordinates (Fig. 4B). Coordinates from their center of masses of the eight sections that are referred to as secondary centers of masses have been calculated (Fig. 4C, Table S1).

Using the coordinates of the eight secondary center of masses and one primary center of mass (Fig.4, Table S1), we have calculated three chirality measures: HCM,[39] Osipov-Pickup-Dunmer chirality indices (OPD)[41], and continuous chirality measure (CCM)[40] (Table 2). The Broyden-Fletcher-Goldfarb-Shano (BFGS) numerical procedure was used to minimize HCM with rotation angle 1°. When calculating CCM, the eight secondary center of masses were assumed to be connected by a 'bond' to the primary center of mass.

The features of the CD spectra correlate with the enumerated chirality measures (Fig. 3C). The sign of the *OPD* shows correlation with the signs of the experimental CD spectrum. HCM and CCM are always positive and provide only an overall quantification of asymmetry. Their values, however correlate with the amplitude of the CD plasmonic peak in the 400–700 nm spectral window (Figs. 1A, 3C).

In conclusion, CPL illumination of a dispersion of plasmonic NPs transfers chirality of photons to the chirality of NP assemblies. The nanoscale products showed opposite chiroptical activities, which depends on the handedness of CPL. Importing tomography coordinates made possible chirality identification and quantification even for assemblies of seemingly irregular shape. Considering the ubiquity of plasmonic properties in NPs, [33,34,43–45] similar synthetic protocols based on the plasmonic inter-particle forces dependent on the light polarization can be applicable to other NPs.

Supplementary Material

Refer to Web version on PubMed Central for supplementary material.

ACKNOWLEDGMENTS

REFERENCES

(1). Lodahl P; Mahmoodian S; Stobbe S; Rauschenbeutel A; Schneeweiss P; Volz J; Pichler H; Zoller P Nature 2017, 541 (7638), 473. [PubMed: 28128249]

(2). Pendry JB Science (80-.). 2004, 306 (5700), 1353.

(3). Ma W; Xu L; de Moura AF; Wu X; Kuang H; Xu C; Kotov NA Chem. Rev 2017, 117 (12), 8041. [PubMed: 28426196]

(4). Kuroda R; Endo B; Abe M; Shimizu M Nature 2009, 462 (7274), 790. [PubMed: 19940849]

(5). Silvera Batista CA; Larson RG; Kotov NA Science (80-.). 2015, 350 (6257), 1242477.

(6). Huck NPM; Jager WF; De Lange B; Feringa BL Science (80-.). 2012, 273 (5282), 1686.

(7). Bailey J Science (80-.). 1998, 281 (5377), 672.

(8). Ayitou AJ-L; Sivaguru J J. Am. Chem. Soc 2009, 131 (14), 5036. [PubMed: 19301904]

(9). Kim J; Lee J; Kim WY; Kim H; Lee S; Lee HC; Lee YS; Seo M; Kim SY Nat. Commun 2015, 6, 6959. [PubMed: 25903970]

(10). Zhong Y; Sisto TJ; Zhang B; Miyata K; Zhu X-Y; Steigerwald ML; Ng F; Nuckolls C J. Am. Chem. Soc 2017, 139 (16), 5644. [PubMed: 28418666]

(11). Noorduin WL; Bode AAC; van der Meijden M; Meekes H; van Etteger AF; van Enckevort WJP; Christianen PCM; Kaptein B; Kellogg RM; Rasing T; Vlieg E Nat. Chem 2009, 1 (9), 729. [PubMed: 21124360]

(12). Müller M; Zentel R Macromolecules 1996, 29 (5), 1609.

(13). Zhang S; Zhou J; Park Y-S; Rho J; Singh R; Nam S; Azad AK; Chen H-T; Yin X; Taylor AJ; Zhang X Nat. Commun 2012, 3, 942. [PubMed: 22781755]

(14). Nikolova L; Todorov T; Ivanov M; Andruzzi F; Hvilsted S; Ramanujam PS Opt. Mater. (Amst) 1997, 8 (4), 255.

(15). Iftime G; Labarthet FL; Natansohn A; Rochon P J. Am. Chem. Soc 2000, 122 (51), 12646.

(16). Feringa BL; van Delden RA Angew. Chemie Int. Ed 1999, 38 (23), 3418.

(17). Yeom J; Yeom B; Chan H; Smith KW; Dominguez-Medina S; Bahng JH; Zhao G; Chang W-S; Chang S-J; Chuvilin A; Melnikau D; Rogach AL; Zhang P; Link S; Král P; Kotov NA Nat. Mater 2015, 14 (1), 66. [PubMed: 25401922]

(18). Toyoda K; Miyamoto K; Aoki N; Morita R; Omatsu T Nano Lett. 2012, 12 (7), 3645. [PubMed: 22690654]

(19). Govan J; Gun'ko YK Nanoscience 2016, 3, 1.

(20). Wang Y; Xu J; Wang Y; Chen H Chem. Soc. Rev 2013, 42 (7), 2930. [PubMed: 23207678]

(21). Guerrero-Martínez A; Alonso-Gómez JL; Auguié B; Cid MM; Liz-Marzán LM Nano Today 2011, 6 (4), 381.

(22). Durán Pachón L; Yosef I; Markus TZ; Naaman R; Avnir D; Rothenberg G Nat. Chem 2009, 1 (2), 160. [PubMed: 21378830]

(23). Saito K; Tatsuma T Nano Lett. 2018, 18, 3209. [PubMed: 29664299]

(24). Boriskina SV; Reinhard BM Nanoscale 2012, 4 (1), 76. [PubMed: 22127488]

(25). Lucas A; Das Sarma S Phys. Rev. B 2018, 97 (11), 115449.

(26). Sawai K; Tatumi R; Nakahodo T; Fujihara H Angew. Chemie - Int. Ed 2008, 120, 7023.

(27). Haruta M Catal. Today 1997, 36, 153.

(28). Gansel JK; Thiel M; Rill MS; Decker M; Bade K; Saile V; von Freymann G; Linden S; Wegener M Science 2009, 325 (5947), 1513. [PubMed: 19696310]

(29). Wu X; Xu L; Liu L; Ma W; Yin H; Kuang H; Wang L; Xu C; Kotov NA J. Am. Chem. Soc 2013, 135 (49), 18629. [PubMed: 24246036]

(30). Hu T; Isaacoff BP; Bahng JH; Hao C; Zhou Y; Zhu J; Li X; Wang Z; Liu S; Xu C; Biteen JS; Kotov NA Nano Lett. 2014, 14 (12), 6799. [PubMed: 25400100]

(31). Kuzyk A; Schreiber R; Fan Z; Pardatscher G; Roller E-M; Högele A; Simmel FC; Govorov AO; Liedl T Nature 2012, 483 (7389), 311. [PubMed: 22422265]

(32). Yan W; Xu L; Xu C; Ma W; Kuang H; Wang L; Kotov NA J. Am. Chem. Soc 2012, 134 (36), 15114. [PubMed: 22900978]

(33). Lee GP; Shi Y; Lavoie E; Daeneke T; Reineck P; Cappel UB; Huang DM; Bach U ACS Nano 2013, 7 (7), 5911. [PubMed: 23730850]

(34). Jin R; Cao Y; Mirkin CA; Kelly KL; Schatz GC; Zheng JG Science (80-.). 2001, 294, 1901.

(35). Kurihara K; Kizling J; Stenius P; Fendler JH J. Am. Chem. Soc 1983, 105 (9), 2574.

(36). Penn RL; Banfield JF Science (80-.). 1998, 281 (5379), 969.

(37). Tang Z; Kotov NA; Giersig M Science (80-.). 2002, 297 (5579), 237.

(38). De Yoreo JJ; Gilbert PUPA; Sommerdijk NAJM; Penn RL; Whitelam S; Joester D; Zhang H; Rimer JD; Navrotsky A; Banfield JF; Wallace AF; Michel FM; Meldrum FC; Cölfen H; Dove PM Science (80-.). 2015, 349 (6247).

(39). Buda AB; Mislow K J. Am. Chem. Soc 1992, 114 (15), 6006.

(40). Zabrodsky H; Avnir D J. Am. Chem. Soc 1995, 117 (1), 462.

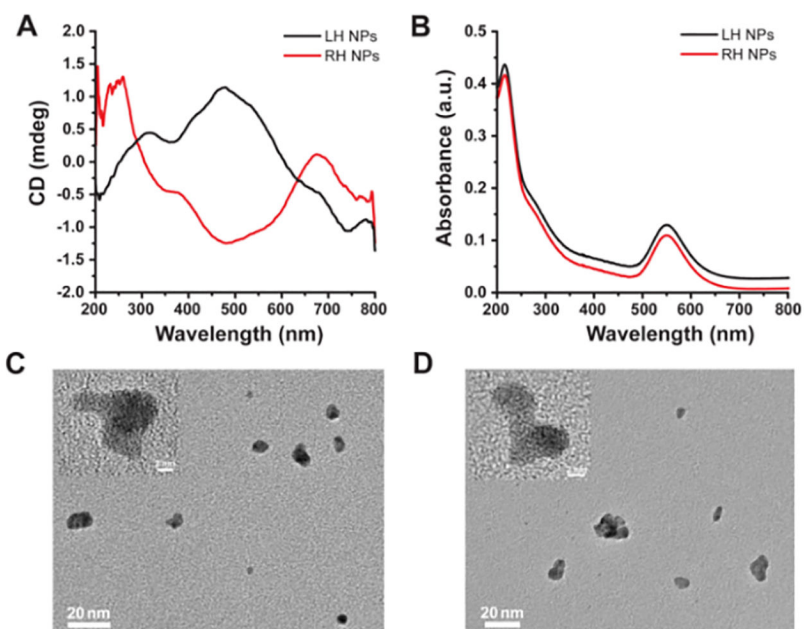(41). Osipov MA; Pickup BT; Dunmur DA Molec. Phys 1995, 84 (August), 1193.

(42). Whetten RL; Garzo IL 2015.

(43). Nanoplates T; Templates S; Generating F; Nanorings T Adv. Mater 2003, 15 (9), 695.

(44). Maillard M; Huang P; Brus L Nano Lett. 2003, 3, 1611.

(45). Zhang J; Langille MR; Mirkin CA J. Am. Chem. Soc 2010, 132 (28), 12502. [PubMed: 20718424]
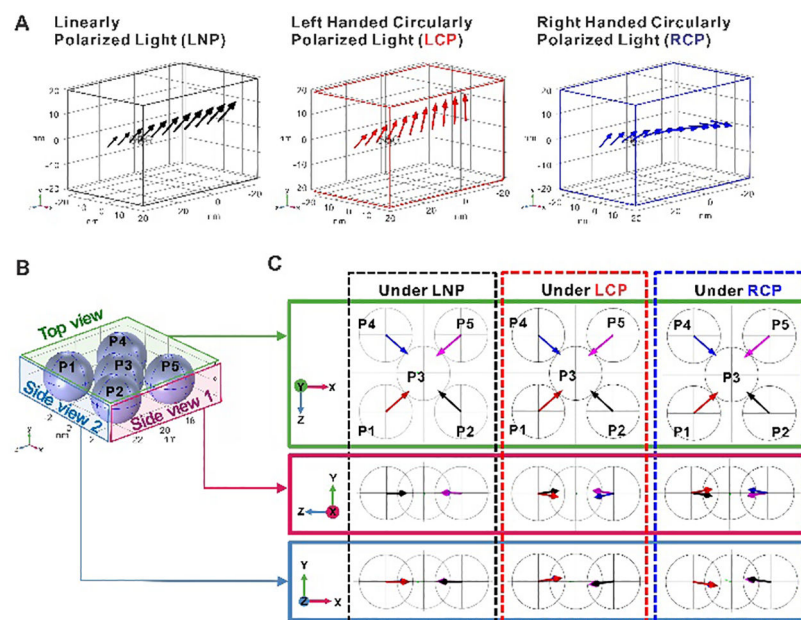
Figure 1. Optical properties and shape of Au NPs after 50 min CPL illumination.
CD (A) and UV-Vis absorbance (B) spectra of nanoscale dispersions illuminated with left-
(LH, black) and right-handed (RH, red) photons. The handedness of the incident CPL
determines the sign of the resulting CD bands. (C, D) HR-TEM images of Au NPs obtained
with LCP (C) and RCP (D), respectively.

Figure 2. Interparticle forces in the achiral plasmonic assemblies dependent on the polarization of incident light.
(A) The forces fields were calculated for three different illumination conditions: linear (black), left-handed circular: (red), and right-handed circular (blue) polarization. The arrows show the directions of electric field of the incident photons as they pass through the nanoassembly (light propagates along the -z direction). **(B)** Model of NP assemblies from five 3 nm gold NPs (P1 to P5). **(C)** Forces acting on each NP (red: P1; black: P2; green: P3; blue: P4; magenta: P5) under three different polarizations light. The arrow lengths are proportional to the magnitude of force on each NP.
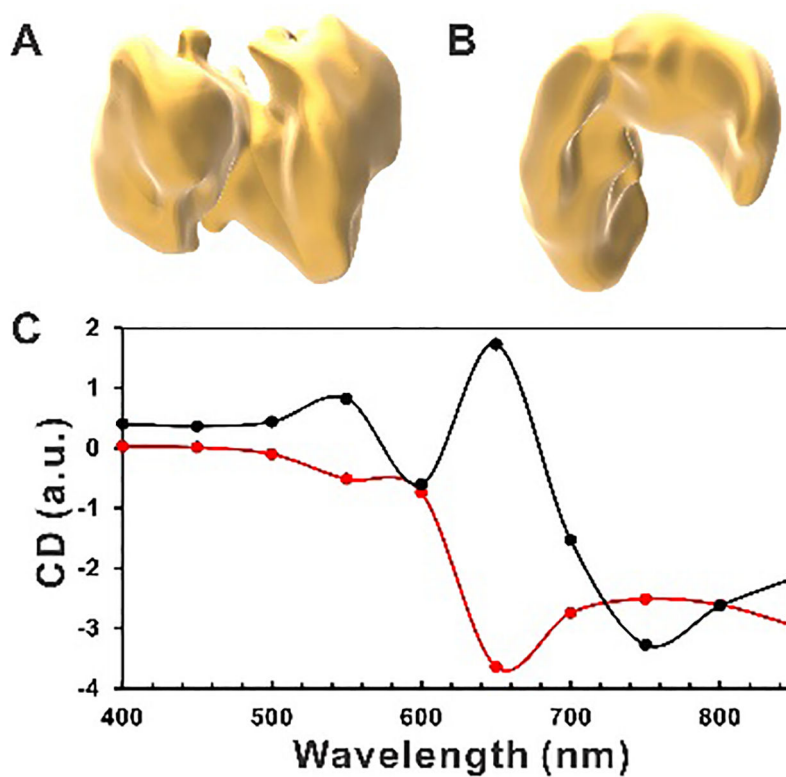
Figure 3.
Electron tomography of Au nanostructures obtained after CPL illumination and their calculated CD spectra. (A, B) Experimentally obtained tomographic reconstructions of LH (A) and RH (B) gold nanostructures formed after illumination with left-handed and right-handed CPL, respectively. (C) Calculated CD spectra with geometry of the particle models imported directly from tomographic reconstructions. (LH: black; RH: red)
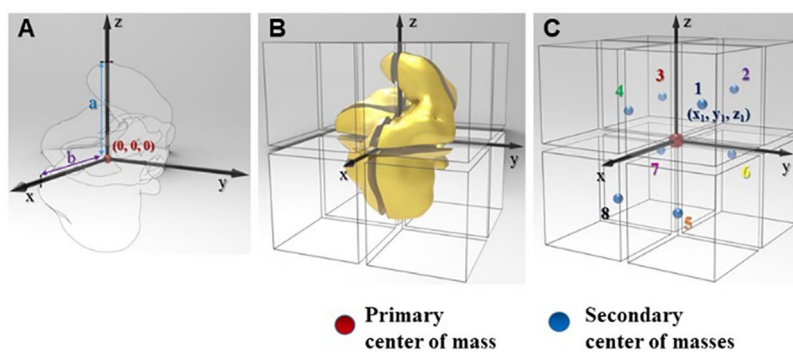
Figure 4. Schematic description of chirality quantifications based on tomographic data for nanoscale structures of arbitrary shape using LH nanoassemblies from Figure 3.
(**A**) Placement of the particle in a Cartesian coordinate system having an origin at the center of total mass. (**B**) Sectioning NPs with the eight octants of coordinate system (**C**) Generating the center of mass from eight different partitions.

Table 1.

Calculated plasmonic forces on each gold NP. The origin of vectors are at the center of each particle (see SI).

Total force acting on each particle vector, unit: N)						
		P1	**P2**	**P3**	**P4**	**P5**
LNP	x	4.26E-19	−4.1E-19	−1.3E-19	3.99E-19	−4.5E-19
	y	−1.8E-21	−1.6E-23	−1.1E-20	1.03E-20	7.61E-21
	z	−3.7E-19	−3.7E-19	−1.5E-20	3.42E-19	3.74 E-19
LCP	x	4.31E-19	−4.1E-19	−1.4E-19	4.01E-19	−4.5E-19
	y	5.97E-20	−5.2E-20	−1.9E-21	6.99E-20	−5.5E-20
	z	−3.7E-19	−3.8E-19	−1.5E-20	3.46E-19	3.77E-19
RCP	x	4.33E-19	−4.1E-19	−1.3E-19	3.99E-19	−4.5E-19
	y	−6.8E-20	5.59E-20	3.94E-20	−6.2E-20	5.08E-20
	z	−3.7E-19	−3.7E-19	−2E-20	3.45E-19	3.66E-19

Table 2.

Chirality quantification for RH and LH Au nanostructures formed after illumination with right-handed and left-handed CPL.

	LH Au NP	RH Au NP
Osipov-Pickup-Dunmur Chirality Index (OPD)	0.6493	−4.965
Hausdorff Chirality Measure (HCM)	0.1343	0.1861
Continuous Chirality Measure (CCM)	1.315	1.738